JCIM JOURNAL OF CHEMICAL INFORMATION AND MODELING

pubs.acs.org/jcim Article

CHARMM Force-Field Parameters for Morphine, Heroin, and Oliceridine, and Conformational Dynamics of Opioid Drugs

Thomas Giannos,◆ Samo Lešnik,◆ Urban Bren, Milan Hodošček, Tatiana Domratcheva, and Ana-Nicoleta Bondar*

Cite This: J. Chem. Inf. Model. 2021, 61, 3964−3977 Read Online

ACCESS | Metrics & More | Article Recommendations | Supporting Information

ABSTRACT: Opioid drug binding to specialized G protein-coupled receptors (GPCRs) can lead to analgesia upon activation via downstream G_i protein signaling and to severe side effects via activation of the β-arrestin signaling pathway. Knowledge of how different opioid drugs interact with receptors is essential, as it can inform and guide the design of safer therapeutics. We performed quantum and classical mechanical computations to explore the potential energy landscape of four opioid drugs: morphine and its derivatives heroin and fentanyl and for the unrelated oliceridine. From potential energy profiles for bond twists and from interactions between opioids and water, we derived a set of force-field parameters that allow a good description of structural properties and intermolecular interactions of the opioids. Potential of mean force profiles computed from molecular dynamics simulations indicate that fentanyl and oliceridine have complex energy landscapes with relatively small energy penalties, suggesting that interactions with the receptor could select different binding poses of the drugs.

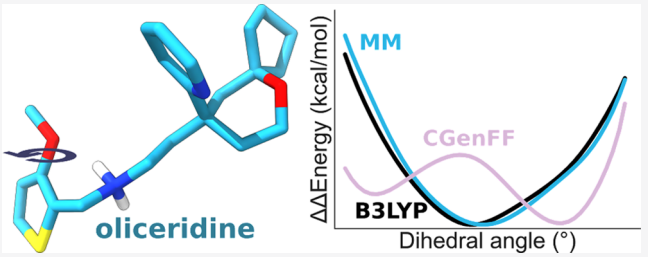

INTRODUCTION

Opioid drugs are primarily used for the treatment of acute and chronic pain. Their biological targets, the opioid receptors, are part of the G protein-coupled receptor (GPCR) family.[1] Long-term opioid use is associated with side effects such as nausea, respiratory depression, and physical dependence,[2] which makes it of paramount importance to develop safer opioid drugs.[3] Morphine (Figure 1A) is a natural opioid and one of the oldest known drugs, but its potent analgesic and sedative effects are associated with serious side effects.[4,5] A strategy to increase oral bioavailability and blood−brain barrier penetration of morphine is to mask its polar OH groups, such as via acetylation, which leads to heroin (Figure 1B), an opioid with higher blood−barrier penetration, but highly addictive. Simplifying the morphine structure by removing three rings and phenolic groups led to 4-anilinopiperidine opioids, of which fentanyl is 100 times more potent than morphine, but with high addiction and respiratory depression potential.[6] Unrelated to morphine, oliceridine is an opioid discovered by screening a library of compounds for binding to the mu-opioid receptor;[7] oliceridine is thought to have reduced adverse effects,[8] but respiratory depression has been associated with its usage.[9] Understanding the structural and energetic elements that govern the response of a cell-signaling network to a particular opioid drug is important, as it could guide the development of safer synthetic opioid drugs. Here, we derived force-field parameters that will enable atomistic computations of opioid drug binding to receptors in the cell.

All four opioid drugs we study here have an N-protonated tertiary amino group but are distinguished by their intrinsic flexibility and overall availability for hydrogen(H)-bonding. It was noted that, in the crystal structure, the piperidine ring of morphine (Figure 1A) has "a slightly distorted chair conformation";[10] each of the two hydroxyl groups participates in an intermolecular H-bond, and one of these hydroxyl groups has an additional intramolecular H-bond with the ether oxygen atom[10] (Figure 1A). The crystal structure reporting two heroin molecules in the asymmetric unit indicates that the two molecules have almost identical ring systems but different orientations of acetyl moieties[11] (Figures 1B and S1). As in the case of morphine,[10] the crystal structure of fentanyl (Figure 1C) indicates a slightly distorted chair conformation of the piperidine ring.[12] An experimental crystal structure of oliceridine is yet to be solved; its chemical structure (Figure 1D) suggests that oliceridine hosts the protonated amino group in an environment significantly more flexible than morphine (Figure 1A).

Whether and how differences in local flexibilities and chemical environment of the protonated amino group shape

Received: June 11, 2021
Published: August 5, 2021

https://doi.org/10.1021/acs.jcim.1c00667
J. Chem. Inf. Model. 2021, 61, 3964−3977

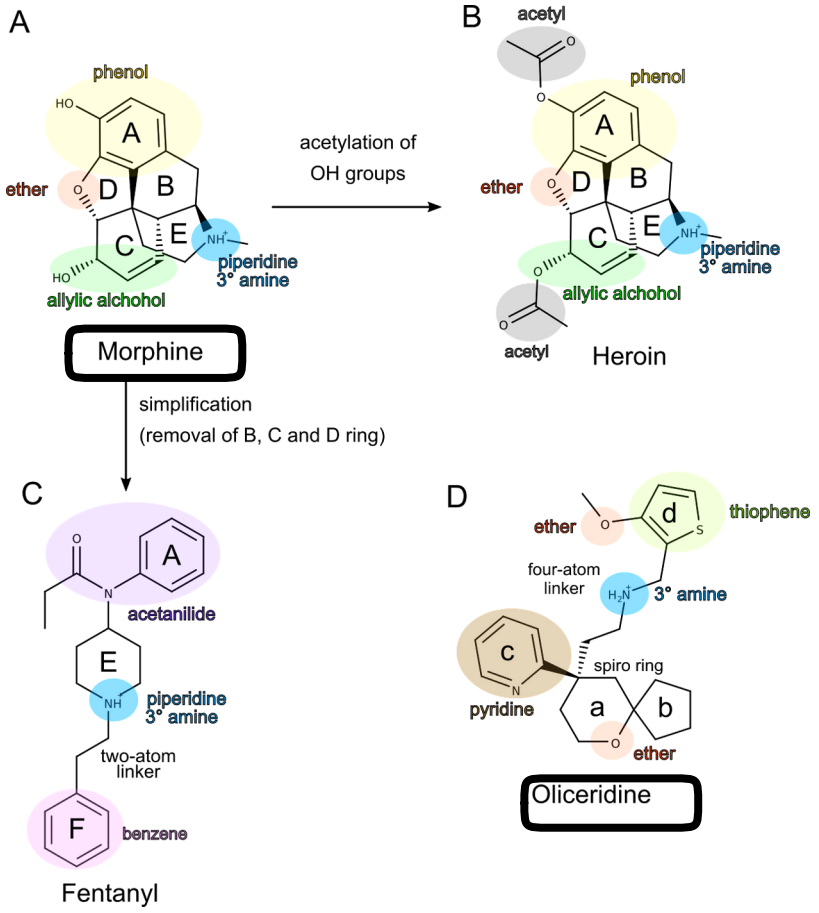

Figure 1. Schematic representation of the four opioid molecules studied here. (A) Morphine contains four functional groups, the positively charged piperidine nitrogen group (blue), the neutral phenolic group (yellow), and the ether (red) and allylic alcohol groups (green). (B) Heroin is a semisynthetic derivative of morphine, acetylated at the OH groups (gray). Structures of heroin-1 and heroin-2 molecules from the starting crystal structure are presented in Figure S1. (C) Fentanyl was obtained by the simplification of the morphine structure, with the removal of rings B, C, and D, and of the OH groups. Fentanyl contains the piperidine nitrogen groups (blue), the benzene (pink) and acetanilide moieties (purple), and a flexible linker region. (D) Oliceridine contains a thiophene group (yellow-green), two ether groups (red), and a pyridine ring (brown). We used MarvinSketch19.4, developed by ChemAxon, to draw chemical structures and Inkscape to add text and color highlights and assemble the panels.

interactions between opioid drugs and their binding partners in the cell are largely unknown. Valuable clues that alterations to the immediate chemical environment can drastically impact interactions at the protonated amino group come from the experimental observation that adding a fluorine atom to fentanyl lowers the pK_a of the compound[13] and from computations indicating that a torsional energy profile for rotation of the piperidine ring is symmetrical in standard fentanyl but pronouncedly asymmetric in the fluorinated derivative.[14]

To characterize torsional energy profiles of opioid drugs, we first used short quantum mechanical simulations to probe motions of morphine, heroin, fentanyl, and oliceridine. Then, based on extensive quantum mechanical computations of potential energy scans (PESs) and water interaction energies, we derived force-field parameters for morphine, heroin, and oliceridine. We relied on the Chemistry at Harvard Molecular Mechanics (CHARMM)[15] general force field (CGenFF) methodology to generate force-field parameters compatible with CHARMM.[16] According to this methodology, force-field parametrization of a druglike molecule involves computations on the entire compound or on fragments of the compound. QM computations are performed to generate target data used as a reference for MM computations. For example, the potential energy profile for the twist around a dihedral angle of the drug molecule is computed with QM and separately with a starting set of MM parameters; the MM parameters are then adjusted to achieve good agreement between the MM and QM profiles. To ensure transferability of the CGenFF parameters, partial atomic charges of the drug molecule are optimized by fitting MM water interaction energies and interaction distances to the HF/6-31G* target data.[16] The accuracy of the MM force-field parameters in describing conformational properties of the drug molecule is tested, e.g., by comparing structures of the compound from QM vs MM geometry optimizations and dynamics.

Using MM parameters presented here, we performed prolonged molecular dynamics (MD) simulations of isolated drug molecules and computed the potential of mean force (PMF) profiles to evaluate structural dynamics. Together with the force-field parameters we presented recently for fentanyl and a fluorinated fentanyl derivative,[14] the parameters reported here establish a framework for atomistic simulations of interactions between opioid receptors and opioid drugs with distinct torsional and H-bond properties.

https://doi.org/10.1021/acs.jcim.1c00667
J. Chem. Inf. Model. 2021, 61, 3964−3977

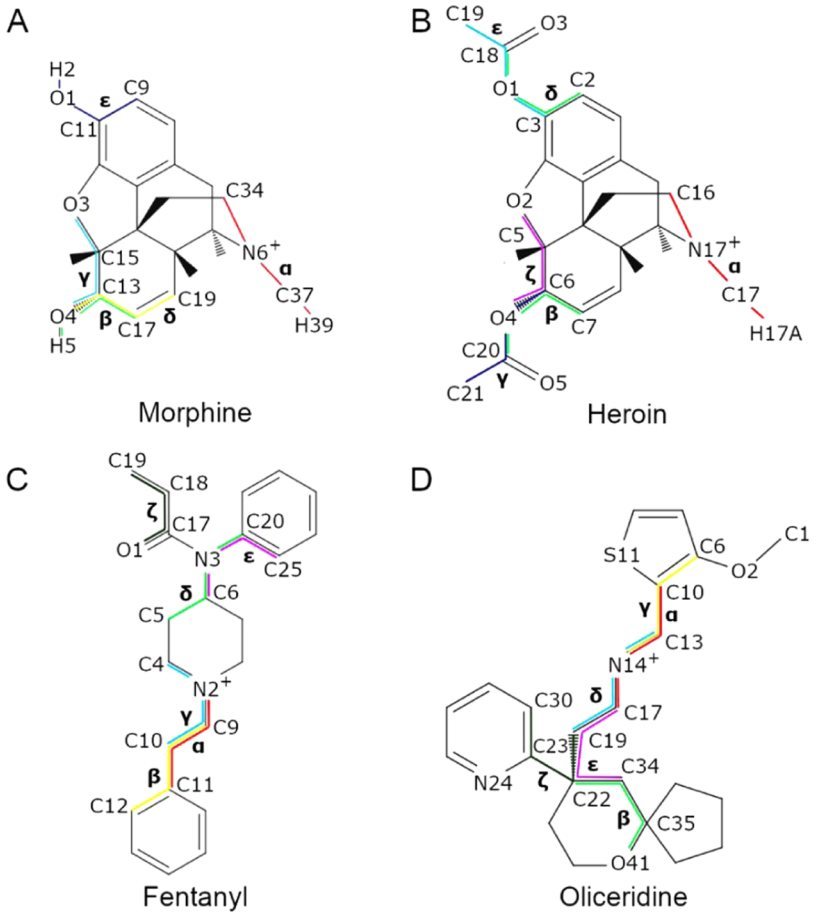

Figure 2. Chemical structures of opioid drugs with selected atom names and dihedral angles marked on the structures. Chemical structures with labels for all atoms are presented in Figure S2. (A–D) Selected atoms and dihedral angles labeled for morphine (A), heroin (B), fentanyl (C), and oliceridine (D). Dihedral angles marked on the structures were used to describe the dynamics of the molecules as sampled with MD simulations.

METHODS

Starting Structures for Isolated Opioid Drug Molecules. Starting coordinates for fentanyl, morphine, and heroin compounds were taken from the corresponding crystal structures,[10−12] and coordinates for oliceridine were generated with Avogadro.[17] Since opioid drugs are typically protonated at the tertiary amine group when binding to the GPCR,[18,19] all four opioid drugs studied here were considered protonated.

The crystal structure of heroin[10] contains two conformers distinguished by the different orientation of the O1−C18 and C18═O3 bonds relative to the remaining of the molecule (Figures 2B and S1); separate computations were performed for both heroin structures, which we denote here heroin-1 and heroin-2 (Figure S1).

QM Geometry Optimizations. The CGenFF protocol recommends that structures of the drug−water molecule complexes used to compute water interaction energies use for the drug molecule a geometry optimized with MP2/6-31G*.[16] Accordingly, for each opioid molecule we parametrized here, we performed a geometry optimization using MP2/6-31G*.

Given the size of the opioid compounds, and the large number of dihedral angles that required optimization of the force-field parameters, MP2 was impractical for computations of PESs for dihedral angles and for QM MD simulations. All dihedral angle PES computations and QM MD were thus performed with B3LYP/6-31G* starting from structures optimized at this level of theory. All geometry optimizations and PES computations were performed with Gaussian 16.[20]

QM MD Simulations. Test MD simulations were conducted using the ab initio molecular dynamics (AIMD) module of ORCA.[21] Initial atomic velocities were assigned according to a Maxwell−Boltzmann distribution at 310 K, which was maintained with a Berendsen thermostat. The time step of the simulations was set to 0.5 fs, and coordinates were written every 10 fs. Simulations were prolonged to ∼57−77 ps for the isolated compounds; given the computational costs, the QM MD simulations for the compounds in the presence of water molecules are shorter, within ∼15−19 ps (Table 1).

Tests for Opioids in Water. We used CHARMM-GUI[22] to generate starting coordinates for opioids in the presence of water molecules. We first placed each B3LYP-optimized opioid structure in the center of a cubic water box and then, for the computations to be amenable to a QM description, we kept only water molecules whose oxygen atom was within 4.5 Å of heavy atoms of the opioid molecule. The resulting systems contained between 134 and 210 atoms (Table 1). Geometry optimizations of opioid molecules in the presence of waters and test MD simulations of these systems were performed with B3LYP/6-31G(d).

Time Series Computed from QM MD Simulations. Root-mean-squared distances (RMSDs) for heavy atoms of heroin and morphine, which are largely rigid molecules, were computed in Visual Molecular Dynamics (VMD)[23] using as a

https://doi.org/10.1021/acs.jcim.1c00667
J. Chem. Inf. Model. 2021, 61, 3964−3977

Table 1. QM Computations of the Dynamics of Opioid Drugs Isolated and in the Presence of Water Molecules[a]

compound	no. of water molecules	no. of atoms	length (ps)
QM MD Simulations for Isolated Opioids			
heroin-1		51	66.31
heroin-2		51	65.84
fentanyl		54	63.26
morphine		41	77.19
oliceridine		58	57.34
QM MD Simulations for Opioids in the Presence of Water			
heroin-1	45	186	15.61
heroin-2	43	180	17.76
fentanyl	52	210	15.15
morphine	31	134	35.74
oliceridine	46	196	19.10

[a]The length of the simulation refers to the production runs. Schematic representations of the opioid drugs are presented in Figure 1. All simulations were initiated from B3LYP-optimized geometries.

reference the atomic coordinates of the starting crystal structures. As fentanyl and oliceridine have highly flexible linkers, we characterized their structural dynamics using selected angles between ring planes.

QM Computations of Potential Energy Scans. Starting from the B3LYP-optimized structures, we used Gaussian[20] v.16 to perform relaxed PES computations for selected flexible high-penalty dihedral angles (Figure 2) with B3LYP/6-31G(d) and a step size of 5°.

MM MD Simulations of Isolated Opioid Drugs. MM MD simulations of the isolated opioid drug molecules were performed with CHARMM[15,16,24,25] v.43b2 using force-field parameters optimized here. All structures were initially minimized using 10 000 steps of steepest descent and adopted basis Newton Raphson, followed by heating using the Nosé–Hoover method[26] and 125 ps equilibration at constant volume with the velocity Verlet integration algorithm. Production runs were performed at constant volume and temperature T = 310 K with the leapfrog Verlet integration scheme for 400 ns.

To compute PMF profiles for dihedral angles of interest, we monitored the time series of the difference between the value of the dihedral angle and the reference value for a dihedral angle in trans (180°) or cis configurations (0°). From histograms of these dihedral angle variations, we computed PMF profiles according to the equation

$$\mathrm{PMF} = -k_B T \ln(N/N_{max}) \quad (1)$$

where k_B is the Boltzmann constant, T = 310 K is the temperature, N_{max} is the count of the preferred value of the dihedral angle variation, and N is the count for each dihedral angle variation.

CHARMM Potential Energy Function and the CGenFF Parametrization Protocol for CHARMM-Compatible Force-Field Parameters. The CHARMM potential energy function[15] is given by a sum of terms describing bonded and nonbonded interactions as follows

$$V(r) = \sum_{\text{bonds}} (b - b_0)^2 + \sum_{\text{angles}} K_\theta(\theta - \theta_0)^2 + \sum_{\text{dihedrals}} K_\varphi(1 + \cos(n\varphi - \delta))^2 + \sum_{\text{impropers}} K_\omega(\omega - \omega_0)^2 + \sum_{\text{Urey-Bradley}} K_S(S - S_0)^2 + \sum_{i=j} \left\{ \varepsilon_{ij} \left[\left(\frac{R_{ij}^{\min}}{r_{ij}} \right)^{12} - 2 \left(\frac{R_{ij}^{\min}}{r_{ij}} \right)^{6} \right] + \frac{q_i q_j}{\varepsilon r_{ij}} \right\} \quad (2)$$

Equation 2 contains terms that depend on the Cartesian coordinates of the molecule being studied and which change during the MM computation and terms denoted as the force-field parameters, which remain unchanged during computations. The force-field parameters for bonded interactions are (i) the force constants k_b, k_θ, and k_φ, which describe the energetic penalties for, respectively, bond stretching, valence angle bending, and bond twisting; (ii) the reference or equilibrium bond length b_0 and equilibrium valence angle θ_0; (iii) the multiplicity n, whose integer values between 1 and 6 describe the number of cycles for a 360° twist of the bond, and the phase δ, with values 0 or 180° used for the location of the minima along the torsional energy profile; (iv) the improper angle term, with parameters k_ω (force constant) and ω_0 (reference value) used to control chirality and planarity of compounds; and (v) the Urey–Bradley term, which uses force constant k_S and reference value S_0 to describe the 1,3-nonbonded interactions of valence angles. The nonbonded interactions between atoms i and j separated by spatial distance r_{ij} consist of the Coulomb electrostatic interactions between atomic partial charges q_i and q_j and van der Waals interactions described as a Lennard-Jones 6-12 potential with well depth ε_{ij} and minimum interaction distance $R_{\min\_ij}$.

CGenFF Force-Field Parametrization Strategy. To be consistent with the CHARMM force field, parameters for a nonstandard drug molecule must be derived according to the CHARMM CGenFF protocol,[16] which consists of an iterative procedure to derive parameters included in the bonded and nonbonded terms of the potential energy function.[16,27,28]

Briefly, the CGenFF parametrization philosophy relies on the selection of appropriate fragments of molecules from CGenFF and QM computations to evaluate the conformational properties of linkers between the fragments and comparison of geometries optimized with QM and MM.[16] The derivation of force-field parameters for equilibrium values of bond lengths b_0 and valence angles θ_0 is based on MP2 geometry optimizations, and force constants for bonded degrees of freedom of heavy atoms are derived from B3LYP computations of potential energy scans.[16] Parameters for van der Waals interactions are transferred from the existing values in the force field.

Partial atomic charges q_i are derived based on computations of water interaction energies. Briefly, for each MP2-optimized geometry of an opioid drug or drug fragment, a water molecule in TIP3P geometry[29] is placed in an idealized H-bonding geometry, at each H-bond donor and acceptor site (Figure 3). For each of these drug–water complexes, the orientation of the water molecule relative to the compound is optimized with HF/6-31G* by keeping fixed all other degrees of freedom,[16] and the QM water interaction energy ΔE_{HF} is computed as

https://doi.org/10.1021/acs.jcim.1c00667
J. Chem. Inf. Model. 2021, 61, 3964–3977

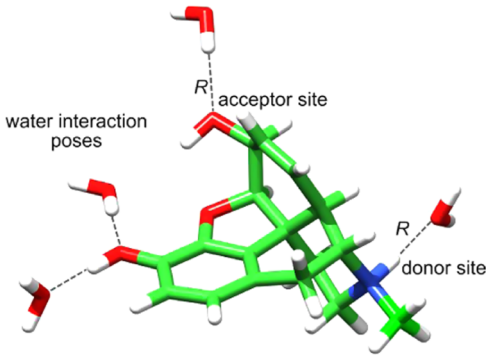

Figure 3. Water interaction sites and water interaction energy computations for optimization of partial atomic charges of morphine. Computations are performed for each accessible H-bond donor and acceptor site. Dotted lines illustrate water interaction distances R calculated separately with QM and MM. Each water interaction was calculated separately.

$$\Delta E_{HF} = E_{HF}(\text{opioid fragment} + \text{water}) - [E_{HF}(\text{opioid fragment}) + E_{HF}(\text{water})] \quad (3)$$

The corresponding QM water interaction distance, R_{HF}, is the distance between the water oxygen atom and the donor/acceptor heavy atom of the opioid drug at the optimized geometry (Figure 3). ΔE_{HF} and R_{HF} are kept unchanged in the case of charged compounds or fragments; in the case of neutral polar compounds, ΔE_{HF} is multiplied by 1.16, and R_{HF} is offset by −0.2 Å.[16] This scaling procedure accounts for limitations of the HF/6-31G(d) description of the drug−water interactions and for the usage of fixed geometries.[16]

MM partial atomic charges were adjusted such that the energy difference $\Delta\Delta E$ between ΔE_{HF} (scaled for polar neutral compounds) and ΔE_{MM}

$$\Delta\Delta E = \Delta E_{HF} - \Delta E_{MM} \quad (4)$$

and the difference between the interaction distances

$$\Delta R = \Delta R_{HF} - \Delta R_{MM} \quad (5)$$

were within the CGenFF convergence criterion of 0.2 kcal/mol for $\Delta\Delta E$.[16] For all H-bond sites of morphine and heroin, we also achieved the convergence criterion of 0.2 Å for $\Delta\Delta R$.[16] In the case of the sulfur atom in oliceridine, we used as convergence criterion for $\Delta\Delta R$ a value of 0.7 Å, as better convergence for the $\Delta\Delta E$ could be obtained only by accepting a lesser convergence criterion for interaction distances.

We used the force-field toolkit plugin[30] of VMD[23] to place a TIP3P water molecule at each of the sterically accessible H-bond donor and acceptor sites of MP2-optimized structures of each compound (Figure 3), Gaussian 16[20] to compute ΔE_{HF} and R_{HF}, and CHARMM for ΔE_{MM} and R_{MM}.

Assignment of Starting Force-Field Parameters. Initial CHARMM bonded and nonbonded parameters were obtained from ParamChem,[27] a Web server that searches for parameters already existing in the CHARMM force field and then reports a penalty value for each parameter. Penalties are assigned based on the similarity of the searched parameter to already existing ones from the CGenFF. The higher the penalty, the lower the confidence in the accuracy of a parameter, such that penalty values ≥10 are considered unreliable. Starting parameters with high penalty values for morphine, heroin, and oliceridine are summarized in Tables S1−S3, respectively.

Parametrization of Partial Atomic Charges of Morphine, Heroin, and Oliceridine. Partial atomic charges of morphine (Figure 1A) were optimized by treating the entire molecule as one fragment. The partial charges of the common rigid structure were transferred from morphine to heroin (Figure 1B), whereas the values of the partial charges of atoms of the acetyl groups of heroin were taken from CGenFF. For oliceridine, given its structure with rigid rings connected by flexible linkers (Figure 1D), we followed the CGenFF recommendation and parametrized separately the partial atomic charges of the methoxythiophene fragment capped with neutral methyl groups (the thiophene Fragment F1 in Figure 4A), whereas for fragments F2, F3, and F4 we kept the original CGenFF partial charges.

Efficient Procedure for Optimization of Partial Atomic Charges. We have recently reported an automated charge-fitting protocol that allowed us to derive a good

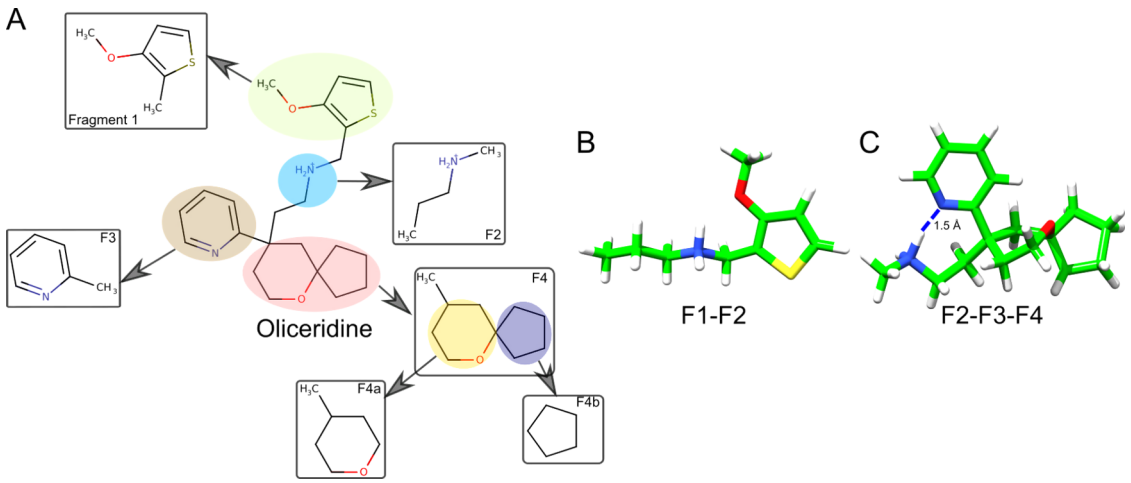

Figure 4. Fragments of the oliceridine molecule used to derive force-field parameters. Each fragment was capped with a methyl group. (A) Fragments F1 and F3 contain ring structures connected by the linker represented with Fragment F2. The spiro ring of oliceridine is represented by fragment F4 and further separated to fragments F4a and F4b. (B, C) Composed fragments used to compute dihedral PES profiles. (B, C) Fragments F1−F2 (B) and F2−F3−F4 (C). In (C), the dotted line indicates intramolecular H-bonding.

https://doi.org/10.1021/acs.jcim.1c00667
J. Chem. Inf. Model. 2021, 61, 3964−3977

description of the partial atomic charges of fentanyl.[14] We used here the same protocol to optimize partial atomic charges for morphine, heroin, and oliceridine. Briefly, the protocol uses a parallelized Python script that relies on the differential evolution algorithm to obtain an initial assessment of the partial charges and then on the sequential least-squares programming (SLSQP) algorithm to refine the charges by minimizing the sum of square differences between ΔE_{HF} and ΔE_{MM}.

As noted before,[31,32] an appropriate choice of the boundary values used in SLSQP computations is essential for reliability of the results. Pursuant to the tests we reported for fentanyl,[14] we allowed the boundary values for the partial atomic charges of oxygen, nitrogen, and sulfur atoms to vary between 0*e* and −1*e*, partial atomic charges of polar H atoms, between 0*e* and 1*e*, and for carbon atoms, between −1*e* and 1*e*.

We have further implemented here as a linear constraint that the sum of all atomic partial-charge values gives the correct integer value of the total charge of the compound. The total charge was set to 1*e* for morphine; the total charge for the oliceridine F1 fragment (Figure 4A) that was parametrized here was set to 0*e*.

Our test computations indicated that once $\Delta\Delta E$ values are within the CGenFF convergence criterion, water interaction distances R also reach convergence. Pursuant to this consideration, we used only $\Delta\Delta E$ values as a convergence criterion for our charge-fitting procedure. Atoms for which the partial charge was optimized here are listed in Table S4. For all other atoms, partial charges were kept as in CGenFF.

RESULTS AND DISCUSSION

We used QM simulations to probe the dynamics of morphine, heroin, fentanyl, and oliceridine. These simulations indicated that the ring structures of morphine and heroin are largely rigid; likewise, the rings of fentanyl and oliceridine are largely rigid, whereas by comparison linker regions are highly flexible. Based on these test simulations, we focused the parametrization of bonded terms on the dihedral angles of the flexible regions. To derive parameters for the Coulomb term of the force field, we performed QM and MM water interaction energy computations for all H-bonding sites of the four opioid drugs and fitted the partial atomic charges for the H-bonding and their directly neighboring atoms within the molecules. Geometry optimizations and test MD simulations indicate that the parameter sets presented here enable a reasonable description of the structural dynamics of the four opioid drugs.

QM-Optimized Structures of Morphine, Heroin, and Oliceridine. For all three compounds, B3LYP- vs MP2-optimized structures are largely the same (Figure 5A,C,D), with RMSD values of the heavy atoms within 0.07−0.3 Å. The MP2-optimized structures of morphine and heroin-2 are also similar to the starting crystal structures in the ring region (Figure 5B,F), whereas the relative orientation of the allylic alcohol groups of morphine (Figures 1A and 5B) and of the acetyl moieties of heroin-1 (Figures 1B and 5E) is somewhat different in the MP2-optimized structure as compared to the starting crystal structure. We suggest that these differences in the relative orientation of flexible groups of morphine and heroin could be due to contributions of intermolecular interactions in the crystal structures, as these interactions are absent in the case of isolated structures optimized with QM.

QM Simulations Indicate Fentanyl and Oliceridine Have Highly Flexible Linkers, whereas Morphine and Heroin Are Largely Rigid Molecules. Our test QM MD simulations indicate that isolated morphine and heroin have relatively small RMSF values for atoms of the ring structure (Figure 6A,C), and average RMSD values are within 0.4 Å (Figures S3−S5). Fluctuations of dihedral angles we inspected are relatively small. For example, most of the time the twist around C13−C15 in morphine remains centered at around −30° (Figure S3H−J) and that for C13−C17 remains around ±180° (Figure S3K−M). The twist around N6−C37 in morphine is most of the time around −60°, with occasional visits to ∼180° (Figure S3B−D); a similar behavior of the corresponding N17−C17 bond twist is observed in heroin-1 (Figure S4C−E). The twist around bond O1−C11 of morphine stays close to 0° (Figure S3N−P); in heroin-1 (Figure S4L−N) and heroin-2 (Figure S5L−N), the corresponding bond twist around O1−C3 is mostly close to ±110°, which could be due to intramolecular interactions between the acetyl moieties of heroin.

Compared to the ring structure, the acetyl groups of heroin-1 and heroin-2 have somewhat larger RMSD values, of up to 2.2 Å (Figures S4B and S5B), and bond twists of these groups show relatively larger fluctuations.

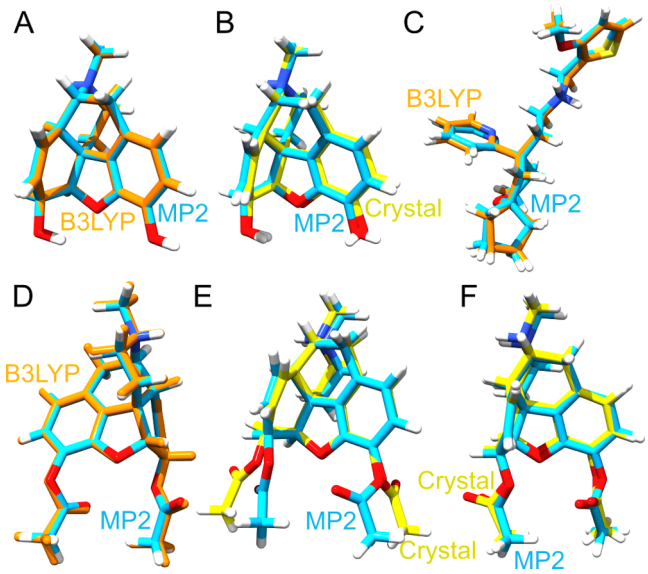

Figure 5. QM-optimized structures of morphine, heroin-1, and oliceridine. Each structure was optimized separately with B3LYP and MP2. For morphine and heroin-1, we compare QM-optimized structures with the corresponding crystal structures. Structures optimized with B3LYP are shown with bonds colored orange, with MP2, in atom color (cyan), and crystal structures are shown with bonds colored yellow. (A) Morphine structures optimized with B3LYP and MP2 are largely identical with a total RMSD of all atoms within 0.1 Å. (B) Except for the twist around the C13−O4 bond, the MP2-optimized structure is in excellent agreement with the starting crystal structure, with RMSD of 0.2 Å. (C) The B3LYP- and MP2-optimized structures of oliceridine are largely the same, with a total RMSD for all atoms within 0.3 Å. (D) The B3LYP- and MP2-optimized structures of heroin-1 are almost identical, with a total RMSD of all atoms within 0.1 Å. (E) The MP2-optimized structure of heroin-1 has an almost identical ring structure as in the crystal structure, but somewhat different orientations of the acetyl moieties, with a total RMSD of 1.1 Å. (F) The MP2-optimized structure of heroin-2 has an almost identical overall structure as is the crystal structure, with an RMSD of 0.3 Å.

https://doi.org/10.1021/acs.jcim.1c00667
J. Chem. Inf. Model. 2021, 61, 3964−3977

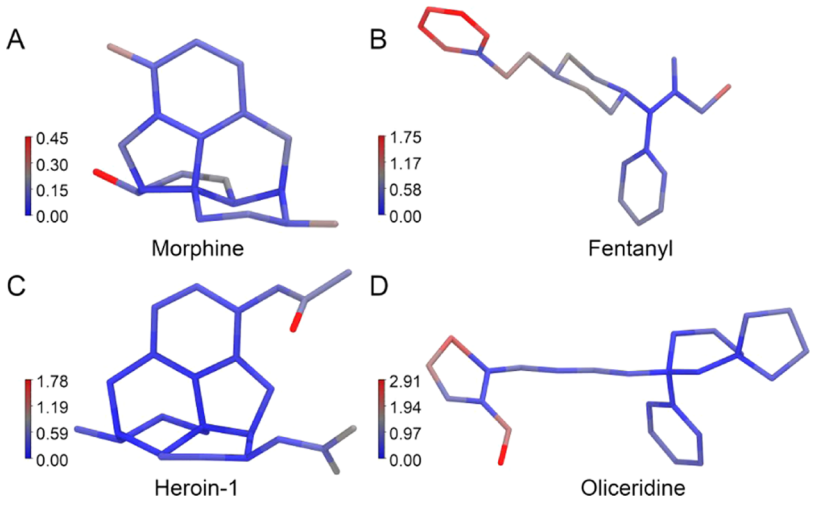

Figure 6. Dynamics of isolated opioid drugs from QM MD simulations. The drug molecules are shown as bonds, with atoms colored according to the RMSF value indicated in the corresponding color bar. (A–D) RMSF values of morphine (A), fentanyl (B), heroin-1 (C), and oliceridine (D). RMSD profiles for isolated morphine, heroin-1, and heroin-2 are presented in Figures S3A, S4A,B, and S5A,B, respectively.

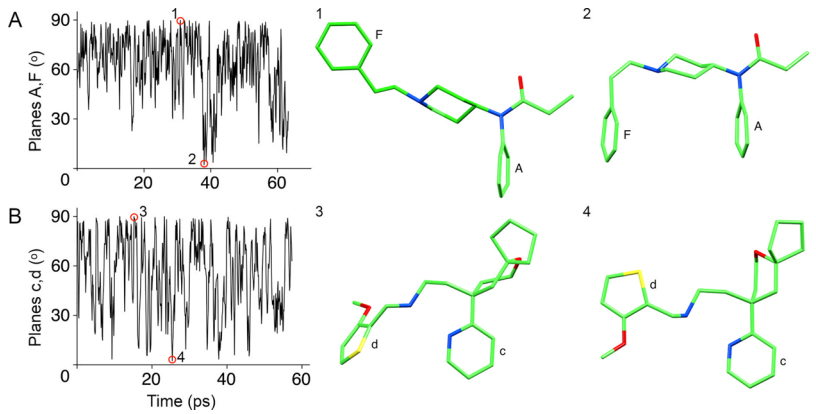

Figure 7. Illustration of the dynamics of the flexible linkers of fentanyl and oliceridine. Additional graphics illustrating the choice of the dihedral angles are presented in Figure S6. For clarity of the profiles, time series of these angles use coordinate sets with a step of 100 fs. Coordinate sets from the time points marked with red circles are illustrated in the corresponding insets. (A) Time series and insets illustrating dynamics of the angle θ between the two benzene rings of fentanyl. (B) Time series and insets illustrating the dynamics of the angle θ between the thiophene and pyridine rings of isolated oliceridine.

As fentanyl and oliceridine have highly flexible linkers that connect ring structures, we characterized their dynamics by monitoring selected dihedral angles (Figures S6 and S7) and angles between ring planes θ—for fentanyl, the angle between the planes of the benzene rings (Figures 7A and S8A), and for oliceridine, the angle θ between the planes of the thiophene and piperidine rings (Figures 7B and S8B). We found that in fentanyl, θ sampled values between 2.2 and 89.9° (inset 1 in Figure 7A); most of the time, isolated fentanyl samples conformations with the two rings oriented at a θ angle of ~62.5 ± 19° and a molecular geometry relatively similar to the B3LYP-optimized structure, in which θ is 53.4°. Conformations whereby the two benzene rings are almost parallel to each other, with $\theta \leq 10°$ (inset 2 in Figure 7A), are sampled only infrequently, <2% of the time.

In the case of oliceridine, θ sampled values between 2.4 and 89.9° (Figure 7B); the average θ value of 55.4 ± 22.4° indicates it is slightly smaller than θ = 77.4° in the B3LYP-optimized structure. Conformations with $\theta \leq 10°$, i.e., with the thiophene and pyridine groups almost parallel to each other, were sampled during <4% of the simulations (inset 4 in Figure 7B). An internal H-bond between the protonated amine group and the nitrogen atom of the pyridine ring is sampled persistently throughout the QM simulations (Figure S9A,C), and it likely contributes to preserving the internal geometry of the linker region (Figure 7B).

The overall picture that emerges from the QM geometry optimizations (Figure 5) and test QM MD simulations (Figures 6 and 7) is that highly flexible linkers connect the ring structures of the opioid drugs. Pursuant to these considerations, we optimized the dihedral angle parameters only for the flexible linkers, as torsional potentials of the linkers likely govern conformational dynamics of the molecules.

Optimization of Partial Atomic Charges of Morphine, Heroin, and Oliceridine. To derive partial charges for morphine, we used as a target the complete morphine molecule and our automated in-house procedure described in the Methods section. We probed water interactions at the sterically accessible heteroatoms O1, O4, H2, and H41 (Figure 2A); during the charge-fitting procedure, we allowed changes in the partial atomic charges of these atoms and of the atoms to which the corresponding functional groups are covalently

https://doi.org/10.1021/acs.jcim.1c00667
J. Chem. Inf. Model. 2021, 61, 3964–3977

bonded. For all sites, $\Delta\Delta E$ values are within 0.2 kcal/mol (Table 2).

Table 2. Water Interaction Energies and Interaction Distances for Morphine

	HF		MM-HF	
atom	ΔE (kcal/mol)	R (Å)	$\Delta\Delta E$ (kcal/mol)	ΔR (Å)
O1	−3.02	3.17	−0.06	−0.29
O4	−3.56	3.05	−0.08	−0.16
H2	−10.93	1.90	−0.12	−0.09
H41	−14.76	1.94	−0.00	−0.15

We transferred the partial atomic charges for the morphine ring and the charged amine group to the corresponding atoms of heroin (Figure 1A,B); for the acetyl groups of heroin, we used the CGenFF partial atomic charges for ethylacetate. To account for the remaining charge after linking the ring structure with the acetyl groups, we adjusted the partial atomic charge of atom C6 (Figure 2B).

Oliceridine was fragmented as presented in Figure 4. Partial charges of atoms of fragment F1 were parameterized by computing water interaction energies according to the standard CGenFF procedure (Table 3). For atoms of fragments F2 and F3, we transferred CGenFF charges from piperidine and 3-methylpyridine, respectively; for atoms of fragments F4a and F4b, we transferred partial charges from CGenGG tetrahydropyran and cyclopentane.

Table 3. Water Interaction Energies and Interaction Distances for the 3-Methoxythiophene Group of Oliceridine[a]

	HF (MP2)		MM-HF (MP2)	
atom	ΔE (kcal/mol)	R (Å)	$\Delta\Delta E$ (kcal/mol)	ΔR (Å)
O2	−2.66	3.27	−0.20	0.74
S11	−0.75	4.00	−0.25	−0.34

[a]Energies were scaled by a factor of 1.16. The interactions energies and distances for the S11 atom were calculated with MP2.

To verify that the partial charges of atoms neighboring the oxygen atom of F4 are correctly described when utilizing the fragment F4a, we used the MP2-optimized structures of F4 and F4a for a Mulliken population analysis. We obtained for the oxygen atom a partial charge of −0.67e when in F4 and of −0.63e when in F4a. Pursuant to this test computation, we consider that the choice of molecular fragments is reasonable.

Optimization of Dihedral Angle Parameters for the Acetyl Moieties of Heroin. All parameters describing flexible dihedral angles of morphine had reasonable ParamChem penalty values (Table S1), and therefore, we kept the original CGenFF dihedral angle parameters. By contrast, in the case of heroin, our ParamChem search reported poor representation of the parameters for the six dihedral angles that describe the orientation of the acetyl moieties (Table S2); we optimized these parameters based on PES computations with B3LYP.

We started from the B3LYP-optimized geometry of heroin-1 (Figure 5D) to perform PES computations with a step of 5°. We used the VMD force-field toolkit and FFTK integrated minimization methods to perform corresponding MM PES computations and to adjust the dihedral angle parameters until the MM PES profiles agreed with B3LYP (Figures 8 and S10).

The twist around the C3−O1 bond of heroin is described by dihedral angles C2−C3−O1−C18 and C4−C3−O1−C18 (Figures 2B and S2B). The B3LYP PES for C2−C3−O1−C18 has energy minima at 122 and 237° and a torsional energy barrier of 5.2 kcal/mol at 182° (Figure S10A). Computing this PES with the original CGenFF parameters gave a profile that lacked the two energy minima (Figure S10A). Likewise, the C4−C3−O1−C18 PES computed with the original CGenFF parameters lacks the energy minima at 66 and 54° (Figure S10B). We added multiplicity terms with values of 1 and 6 to

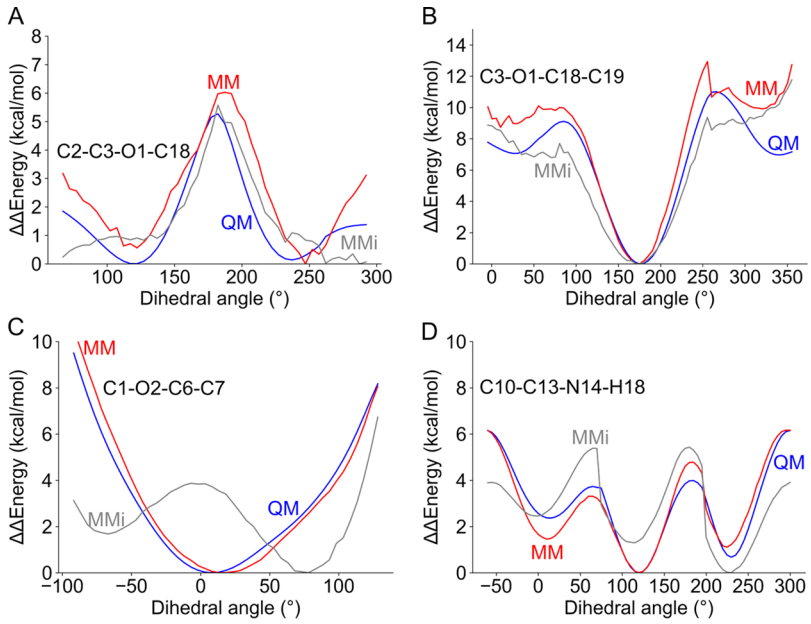

Figure 8. Parametrization of selected dihedral angles of heroin and oliceridine. For each dihedral angle, we compare PES profiles computed with B3LYP (QM, blue curves), with the original CGenFF parameters (MMi, gray curves), and with the CHARMM parameters refined here (MM, red curves). (A, B) PES profiles computed for dihedral angles C2−C3−O1−C18 (A) and C3−O1−C18−C19 (B) of heroin. (C, D) PES profiles computed for dihedral angles C1−O2−C6−C7 (C) and C10−C13−N14−H18 of oliceridine (D).

https://doi.org/10.1021/acs.jcim.1c00667
J. Chem. Inf. Model. 2021, 61, 3964−3977

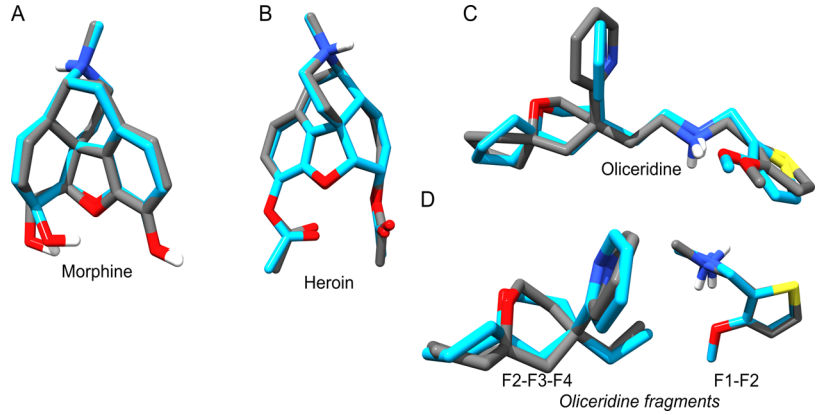

Figure 9. Force-field parameters presented here give a good description of equilibrium structures of opioid drug molecules. Bonds between carbon atoms are colored gray in the MP2-optimized structures and cyan in the MM structures. (A–D) Overlaps between MP2- and MM-optimized structures of morphine (A), heroin-1 (B), oliceridine (C), oliceriding fragment F1–F2, and oliceridine fragment F2–F3–F4 (D).

the description of the C2–C3–O1–C18 dihedral angle and one term with multiplicity value 1 to the C4–C3–O1–C18 dihedral. The resulting PES profiles give a good description of the location of the energy minima (Figure S10A,B). The torsional barriers computed with the refined MM parameters are within 0.7 kcal/mol of the corresponding B3LYP values (Figure S10A,B).

The torsion around the O1–C18 bond of heroin is described by dihedral angles C3–O1–C18–C19 and C3–O1–C18–O3 (Figures 2B and S10C,D). The B3LYP PES profile for C3–O1–C18–C19 has a deep energy minimum at a dihedral angle value of 180°, separated by energy barriers of 9 and 11 kcal/mol from the local energy minima at 26 and 341° (Figure S10C). The original CGenFF parameters give, for both dihedral angles, a PES that lacks the local energy minima and underestimates the energy barriers by ∼1.5–2 kcal/mol.

A similar B3LYP profile and limitations of the original CGenFF parameters are observed for the PES of C3–O1–C18–O3 (Figure S10D). By adding to the description of the dihedral angle C3–O1–C18–O3 one multiplicity term with value 1, we obtained, for both C3–O1–C18–C19 and C3–O1–C18–O3, the local minima of the PES profiles and a good description of the twists associated with energies of up to ∼8 kcal/mol (Figure S10C,D). The energy barriers are overestimated by ∼1–2 kcal/mol relative to B3LYP (Figure S10C,D); since crossing energy barriers of ∼9–11 kcal/mol requires simulation time scales on the order of microseconds, we suggest that the parameters we present here will give a good description of structural dynamics on the submicrosecond time scale.

The twist around the C6–O4 bond is described by dihedral angles C5–C6–O4–C20 and C7–C6–O4–C20 (Figures 2B and S2B), whose B3LYP PES profiles have energy barriers of 15 kcal/mol when the bond is twisted 260°, 8 kcal/mol at −3°, and a shoulderlike energy penalty of 3 kcal/mol at 97° bond twist (Figure S10E,F); the original CGenFF parameters overestimate these energy barriers by 2–7 kcal/mol (Figure S10E,F). Despite this overestimation, our test computations indicated that the original CGenFF parameters allow very good description of the structure, such that the MM- and MP2-optimized structures are very similar to each other (Figure 9B). By contrast, when we adjusted the MM parameters to improve the overlap between the MM- and B3LYP PES profiles, the agreement between the MM- and MP2-optimized structures worsened (Figure S11). We thus kept the original CGenFF parameters for C5–C6–O4–C20 and C7–C6–O4–C20.

Optimization of Dihedral Angle Parameters Oliceridine. Our ParamChem search indicated high penalty scores for dihedral angles of the flexible 4-atom linker of oliceridine, for the thiophene group, and for the ether moiety (Table S3). For the twist around the C10–C13 bond of the thiophene ring, for example, ParamChem gives scores >100, indicating a rather poor description of this bond twist (Figure 2D and Table S3). To derive parameters for dihedral angles of oliceridine, we relied on the combined fragments F1–F2 (Figure 4B) and F2–F3–F4 (Figure 4C), as they contain all dihedral angles of interest. We then used the combined fragment F2–F3–F4 (Figure 4C) to explore the impact of the intramolecular H-bond that was observed in the test QM MD simulations of isolated oliceridine (Figure S9A).

Dihedral angle C1–O2–C6–C7 gives the orientation of the ether chain relative to the thiophene group (Figures 1D and 2D). The B3LYP PES profile for C1–O2–C6–C7 is rather shallow, with an energy minimum at 8° and energetic penalties of ∼6 kcal/mol for bond twists of up to ∼100° (Figures 8C and S12A); there are no local minima on the B3LYP PES profile of C1–O2–C6–C7. Instead of a minimum, the CGenFF parameters give an energy barrier at an angle of 0° and minima at ±75° (Figure S12A). To correct the description of C1–O2–C6–C7, we set to zero the original term with multiplicity 4 and, for the remaining term with multiplicity 2, we increased the energy barrier from 1.58 to 2.084 kcal/mol. The resulting MM PES profile for C1–O2–C6–C7 agrees very well with the B3LYP counterpart (Figures 9C and S12A).

The orientation of the thiophene group relative to the remaining of the molecule is described by the twist around the C10–C13 bond and thus by dihedral angles C6–C10–C13–N14, S10–C10–C13–N14, and S10–C10–C13–H16 (Figures 1D and 2D). The B3LYP PES profile for C6–C10–C13–N14 indicates an energy minimum at 56° and energy barriers of 4 and 8 kcal/mol at 0 and −180°, respectively (Figure S12B). The PES profile obtained with the original CGenFF parameters underestimates by ∼3.7 kcal/mol the energy barrier at 0°, and it overestimates by ∼2 kcal/mol the energy barrier at 180° (Figure S12B). Similar observations can be made for the PES profiles we computed for S10–C10–C13–N14 (Figure S12C) and S10–C10–C13–H16 (Figure S12D). To correct the description of the C10–C13 bond twist, we

https://doi.org/10.1021/acs.jcim.1c00667
J. Chem. Inf. Model. 2021, 61, 3964–3977

removed from the parameters of C6−C10−C13−N14 the term with multiplicity 1 and added to S11−C10−C13−N14 a term with multiplicity 1 and energy barrier of 4.204 kcal/mol. This led to a very good description of all three dihedral angles for the C10−C13 bond twist (Figure S12B−D).

Dihedral angles C10−C13−N14−H18 and C10−C13−N14−C17 are important for the orientation of the protonated amine group relative to the remaining of the oliceridine molecule (Figures 1D and 2D). The B3LYP profile indicates that relatively small energy barriers of 3.5−4 kcal/mol separate the lowest-energy minimum at 120° from the local minima at 10 and 225° (Figure S12E). By contrast, the original CGenFF parameters indicate the lowest-energy minimum at 230°, separated by an energy barrier of ∼5.5 kcal/mol from the local minimum at 180° (Figure S12E). We added to the description of the C10−C13−N14−H18 dihedral angle a multiplicity term with value 1 and energy barrier of 2.352 kcal/mol and increased the energy barrier of the term with multiplicity 3 from 0.04 to 0.286 kcal/mol. For the dihedral angle C10−C13−N14−C17, we kept the values found with ParamChem for the fragment F1−F2 (Figure 4B). With these parameters, we obtained a correct location of the local minima and local energy barriers and an excellent description of the lowest-energy minimum at 120° (Figure S12E,H).

The dihedral angle C17−C19−C22−C23 describes dynamics of the flexible linker relative to the pyridine ring of oliceridine (Figure 1D and 2D). The B3LYP PES profile has a minimum at −70°, and it is somewhat shallow, such that twisting the C19−C22 bond by ∼60° costs ∼10 kcal/mol (Figure S12F). The CGenFF profile indicates the energy minimum at −80° and, for clockwise twists, a steeper energy increase (Figure S12F). When we removed the term with multiplicity 3 and added a term with multiplicity 1 and an energy barrier of 2.542 kcal/mol, we improved somewhat the description of the clockwise twists around the C19−C22 bond but obtained a somewhat worse description of the counter-clockwise twists. Importantly, these changes to the C17−C19−C22−C23 parameters led to an improved description of the oliceridine dihedral angles described above.

The twist around the C22−C23 bond gives the relative orientation of the pyridine and spiro rings of oliceridine (Figures 1D and 2D). To optimize the description of the C19−C22−C23−N24 dihedral angle, we removed the term with multiplicity 2 and added instead a term with multiplicity 3 and an energy barrier of 0.38 kcal/mol (Figure S12G).

The B3LYP-optimized structure of the F2−F3−F4 fragment indicates an intramolecular H-bond between atoms N14 and N24 of the pyridine ring (Figure 4C). Whereas a H-bond between N14 and N24 is absent from the B3LYP-optimized structure of the complete oliceridine molecule, it is established quickly, within picoseconds, during both QM and MM simulations of isolated oliceridine (Figure S9A,C), and it remains present throughout the entire-short-QM simulation; in the prolonged MM simulation, the H-bond breaks and reforms on the nanosecond time scale (Figure S9D). When water molecules are included in the QM MD, instead of a direct H-bond, N14 and N24 prefer to interact with water (Figure S9B,C). We suggest that, during MD simulations of oliceridine in the presence of a membrane-embedded receptor, sampling of oliceridine conformations with an intramolecular H-bond might depend on how much water is present inside the receptor.

MM-Optimized Structures of Morphine, Heroin, and Oliceridine. To ascertain the accuracy of the parameters we derived for describing equilibrium structures of the opioid drugs, we compared geometries optimized with MP2 vs with the MM parameters we derived. Structure overlaps illustrated in Figure 9 indicate excellent agreement between MP2 and MM for the rigid ring regions of morphine and heroin and good agreement for their flexible moieties (Figure 9A,B); the overall RMSD computed for all heavy atoms is 0.3 Å for morphine and 0.4 Å for heroin. For the complete oliceridine molecule, we obtain an RMSD of 1.1 Å, which is explained by limitations of our force-field parameters in describing the relative orientation of ring structures (Figure 9C). Indeed, when we minimize separately fragments F1−F2 and F3−F4 of oliceridine, we obtain close structure overlaps (Figure 9D) and RMSD values of 0.9 and 0.3 Å, respectively. We conclude that the parameters we derived here give good description of the structures of the three opioid drugs.

Prolonged MM Simulations of Isolated Drug Molecules. We used prolonged MM MD simulations to probe the dynamics of isolated opioid drugs. We monitored the time series of the values sampled by dihedral angles we parametrized, calculated histograms to inspect the distribution of these dihedral angle values, and then used eq 1 to compute MM PMF profiles. PMF values in regions with poor sampling of dihedral angle values were removed as unreliable, and we focused instead on valley regions of the PMF in which sampling was adequate. We compared MM vs QM time series of selected dihedral angles from simulations of the isolated drug molecules and MM PMF profiles with the corresponding B3LYP PES profiles. As summarized briefly below and illustrated in Figures S13−S25, the parameters we present here describe well the relatively small bond torsions sampled on the time scale of the simulations we performed.

Overall, time series (Figure S13), histograms (Figure S14), and PMF profiles (Figure S15) computed for dihedral angles of morphine indicate values compatible with the number and location of stationary points along the corresponding PES profiles. The dihedral angle C34−N6−C37−H38 visits periodically the minima observed along the PES (Figure S15A). Despite the simulation being relatively long and the torsional barrier of N6−C37 below <3 kcal/mol, sampling of transient events in which the molecule jumps among energy minima is poor, leading to unreliable values of energy barriers in the MM PMF profile (Figure S15A).

For the dihedral angle C17−C13−O4−H5 of morphine, we observe that the molecule does spend time in the conformation where the dihedral angle value is close (∼45°) to the lowest-energy minimum of the QM PES (∼30°). However, the lowest-energy value in the MM PMF is at ±180°, where the QM PES is unfavorable (Figure S15B). This difference between the MM PMF and QM PES for C17−C13−O4−H5 is associated with shifts in the positions of the energy minima for O3−C15−C13−O4 and C19−C17−C13−O4 (Figure S15C,D). We inspected the MM trajectory and found that atom O4 H-bonds to the aromatic group −O1H (Figure S16), which likely provides favorable energy to shape the energy landscapes for the dihedral angles above.

Dihedral angles we inspected from the MM dynamics of heroin-1 (Figures S17 and S18) indicate the flexible moieties of the molecule sample conformations compatible with the intrinsic torsional profiles. For example, C16−N17−C17−H15 samples periodically value around 0° and ±130° (Figures S17A

https://doi.org/10.1021/acs.jcim.1c00667
J. Chem. Inf. Model. 2021, 61, 3964−3977

and S18A), which agree well with the location of the minima in the corresponding PES (Figure S19A). For C7−C6−O4−C20, C6−O4−C20−C21, and C3−O1−C18−C19, which have relatively steep PES profiles, sample values close to their equilibrium values (Figures S17B,C,E, S18B,C,E, and S19B,C,E). Dynamics of C2−C3−O1−C18 is somewhat different in MM MD as compared to B3LYP PES: whereas on the PES profile the minima at 0 and 130° are isoenergetic, in MM MD the local minimum at 130° is sampled much more often than that at 0° (Figures S17D and S19D); this difference in the energy profile of C2−C3−O1−C18 is associated with a shift in the energy minimum for O2−C5−C6−O4 from ∼40° in the B3LYP PES to ∼10° in MM MD (Figure S19F). In the B3LYP PES at 0°, the acetyl groups are far apart, with a carbonyl oxygen distance of 4.6 Å, whereas in the MM dynamics, this average distance is 3.8 Å and can be as low as 2.8 Å when the value of the C2−C3−O1−C18 dihedral angle is close to 0° (Figure S19G,H). Therefore, on average, we observe a stronger repulsion due to the proximity of acetyl oxygen atoms and larger fluctuations of the dihedral angle during MM dynamics.

The flexible linkers of oliceridine have dihedral angles that fluctuate rapidly during MD (Figures S20 and S21). For C6−C10−C13−N14, S11−C10−C13−H16, and S11−C10−C13−N14, the MM simulation samples well the region between about −60 and 180°, where energy barriers between minima at ∼0 and 135° are ∼5 kcal/mol (Figure S22B−D); for each of these three dihedral angles, transitions to values of ∼about −180° are energetically more costly, ∼8 kcal/mol, and thus poorly sampled on the time scale of our simulations. For C1−O2−C6−C7, we obtain rapid fluctuations during MM MD, with an associated shallow PMF profile (Figures S20A, S21A, and S22A). The MM PMF profile of C10−C13−N14−C17 has the three local minima anticipated from the B3LYP PES, but in the MM PMF, the minima at −90 and 130° are isoenergetic and ∼0.5 kcal/mol below the minimum at ∼0°; by contrast, the B3LYP PES profile favors the minimum at 0° by ∼1 and ∼2.5 kcal/mol relative to the minima at 135 and −90° (Figure S22E). For C17−C19−C22−C23 and C19−C22−C23−N24, we observe a wider range of values sampled in the MM MD as indicated by the B3LYP PES for torsional values <10 kcal/mol (Figure S22F,G). As two of the dihedral angles for which we observe qualitatively different MM PMF vs B3LYP PES profiles include atoms N14 and N24, we suggest that the differences reflect the interplay between the intrinsic torsional potential, parametrized with B3LYP PES, and the intramolecular interactions, such as H-bonding between N14 and N24 (Figure S9), that are only captured by the MM simulation of the complete molecule.

For completeness, we performed an MM MD simulation of the isolated fentanyl molecule using the force-field parameters we presented recently[14] and compared the MM PMF profiles with the corresponding B3LYP PES used in the original parametrization.[14] The flexible dihedral angles sample values in good qualitative agreement with the corresponding B3LYP PES profiles (Figures S23−S25) although transitions between energy minima tend to be relatively poorly sampled on the time scale of the MM simulations.

Fentanyl dihedral angles C4−N2−C9−C10, C5−C6−N3−C20, C11−C10−C9−N2, and C12−C11−C10−C9 (Figure 1C) have complex B3LYP PES profiles with several stationary points (Figure S25A,B,D,E), and C19−C18−C17−O1 has a shoulder on each side of the energy minimum (Figure S25F). The MM PMF of C4−N2−C9−C10 is in good qualitative agreement with B3LYP PES although the MM PMF is shallower for dihedral angle change values from ∼0 to ∼90°, i.e., fluctuations of this dihedral angle are energetically less costly in MM than in the B3LYP PES (Figure S25A).

For C11−C10−C9−N2, the three local minima along the MM PMF are at dihedral angle values close to the B3LYP PES (Figure S25D); the lowest-energy local minima at about −135 and −5° in the B3LYP PES remain as such in the MM PMF; however, in the MM PMF, the B3LYP local minimum at ∼130° is shifted to ∼110° in MM, and it is easily accessible (Figure S25D).

At the protonated amine group of fentanyl, changes of dihedral angle C5−C6−N3−C20 from ∼10 to about 80° are largely isoenergetic in the B3LYP PES, and this region of the PES is ∼2.5 kcal/mol above the lowest-energy minimum at ∼135° (Figure S25B). In the MM PMF, the region of a largely isoenergetic change of the dihedral angle is restricted to the range of ∼15−60°, and this range of dihedral angle values corresponds to the lowest-energy region of the PMF, ∼0.5 kcal/mol below the local minimum at 135° (Figure S25B).

The dihedral angle C6−N3−C20−C21 of fentanyl has a simple B3LYP PES profile with a single energy minimum at 0° and a relatively steep energy increase when the dihedral angle is scanned, such that a 45° value of the dihedral angle is associated with an energetic penalty of ∼4 kcal/mol, and 60°, about 6 kcal/mol (Figure S25C). The MM PMF profile of C6−N3−C20−C21 has an energy minimum at 0°; however, it is shallower, such that a 45° value of the dihedral angle costs only ∼1 kcal/mol, and 60°, ∼4 kcal/mol (Figure S25C).

Inspection of the MM simulation trajectory indicates that differences between dihedral angles of the flexible linker region in MM MD vs B3LYP PES are associated with the sampling, during the MM MD simulation, of an intramolecular H-bond between the protonated amino nitrogen atom N2 and the oxygen atom O1 of the acetanilide moiety (Figures 1C, 2C, and S25G). Thus, for both fentanyl and oliceridine molecules, intramolecular H-bonding at the protonated amino group shapes the conformational dynamics of the isolated molecule.

Test QM MD Simulations of Opioid Drugs in the Presence of Water Molecules. Intermolecular interactions of the protonated amine group could impact binding to the opioid receptor. The transmembrane region of opioid receptors can be visited, at least transiently, by water molecules that interact with protein groups within an extensive H-bond network;[33] an opioid drug binding to the receptor is thus likely to experience a polar, dynamic environment in which it will interact with a fluctuating H-bond network. As a first step toward characterizing putative interactions between opioid drugs and water, we performed short B3LYP/6-31G* MD simulations of morphine, heroin, oliceridine, and fentanyl, in the presence of water molecules. Given the relatively large number of electrons of the simulation systems composed of an opioid drug and water molecules, the number of basis functions is large and thus the simulation times we report are somewhat short. In spite of this limitation, the QM MD simulations provide clues about water−drug interactions and thus complement the water interaction energy computations performed according to the standard CGenFF parametrization protocol.

We monitored, for each oxygen and nitrogen atom of each molecule, the minimum distance to a water oxygen atom (Figures S26−S31). For a direct comparison between B3LYP

https://doi.org/10.1021/acs.jcim.1c00667
J. Chem. Inf. Model. 2021, 61, 3964−3977

values for water interaction distances and values from the HF computations for water interaction energies, in the case of heroin, we restrict ourselves to heroin-1, which we used for force-field parametrization (Figure 9B).

Results summarized in Table 4 indicate that H-bonds with relatively short interaction distances are sampled at all H-bonding sites. Overall, the average absolute differences between the minimum opioid−water distances from B3LYP MD test simulations and the corresponding HF values between an opioid atom and a water oxygen atom are within 0.3 Å (Table 4). The protonated nitrogen atoms of the four opioid drug molecules have particularly stable interactions with a water molecule that remains, in each simulation, within about 2.7−2.8 Å from the nitrogen atom (Figures S26A,E,K,Q,S, S27A, S28A, S29A, S30A, and S31A and Tables 4 and S4).

Table 4. Water Interaction Distances in B3LYP MD Simulations vs Water Interaction Energy Computations[a]

	distance (Å)		
atom	MD B3LYP/water O atom	HF/water O atom	HF/water H atom
	Morphine		
O1	2.6 ± 0.1	3.2	2.2
O3	3.1 ± 0.2	3.2	2.3
O4	2.7 ± 0.1	3.1	2.1
N6	2.8 ± 0.1	3.0	1.9
	Heroin-1		
O1	3.2 ± 0.2	3.2	2.2
O2	2.9 ± 0.2	3.1	2.1
O4	3.1 ± 0.2	3.2	2.2
N17	2.7 ± 0.1	3.0	1.9
O3	2.9 ± 0.1	3.8	2.9
O5	2.9 ± 0.2	3.0	2.0
	Oliceridine		
N14	2.8 ± 0.1	2.9	1.9
N24	3.0 ± 0.2	4.0	3.0
O41	3.0 ± 0.2	3.0	2.0
O2	3.4 ± 0.4	3.2[b]	2.3[b]
S11	3.6 ± 0.4	3.8[b,c]	2.8[b,c]
	Fentanyl		
N2	2.8 ± 0.1	3.0	1.9
O1	2.8 ± 0.2	3.0	2.0

[a]We report average values for the minimum distance between an oxygen or nitrogen atom of the opioid drug and any water molecule; all averages were computed from the last 10 ps of each simulation. We compare these values to distances obtained during water interaction energy computations for optimization of partial atomic charges. Atom names are indicated in Figures 2 and S2. Additional values for interactions between water and heroin-2 in B3LYP MD computations are summarized in Table S5. The protonated nitrogen atom of each opioid drug molecule is in bold. [b]Calculated using oliceridine fragment F1. [c]Calculated using MP2 for convergence of water interaction energy computations.

For atoms O3 of heroin-1 (Figure S28D) and atom N24 of oliceridine (Figure S31B), the minimum distance to a water oxygen atom in B3LYP MD is ∼0.9−1 Å shorter than in the corresponding HF geometry optimization. As detailed below, we suggest that these discrepancies are due to differences in intramolecular interactions of flexible moieties that host these two atoms.

Atom O3 of both heroin-1 (Table 4 and Figure S28D) and heroin-2 (Table S5 and Figure S29D) is within 2.9−3.0 Å distance of a water molecule during test B3LYP MD simulations, as compared to 3.8 Å in the HF-optimized structure (Table 4). Atom O3 is part of a flexible acetyl moiety; during dynamics, an increase in the relative distance between the heroin's acetyl moieties enables a shorter water interaction distance (Figures S28D and S29D). Atom N24 of oliceridine is part of the pyridine ring (Figure 1D); as recommended by the CGenFF protocol, water interaction energies of selected oliceridine atoms were computed using fragments. In these computations, the short water interaction distance for N24 was hindered by interactions between water and the nearby ether oxygen atom O41 (Figures 1D, 4, and S2D). During B3LYP MD on the complete molecule, the pyridine ring can rotate, which allows atom N24 to interact closely with a water molecule (Table 4 and Figure S31B). For O41, water interaction distances are very similar in B3LYP MD and HF optimization (Table 4).

Throughout the QM MD simulations, water can transiently approach other sites that are sterically accessible, such that, on average, there are about 16−25 water molecules within 4.5 Å of each of the four drug molecules (Figure S32); of these water molecules, on average, at any given time, 5−6 waters are within the H-bond (3.5 Å) distance of morphine and oliceridine, 2 waters are within the H-bond distance of fentanyl, and 9 waters are within the H-bond distance of heroin-1 (Figure S32). Although the somewhat short time scales we could achieve for QM MD simulations make it difficult to conclude on the precise pattern of hydration of the opioid drug molecules, we interpret the results here to suggest that, most likely, the opioid drug molecules could have, simultaneously, multiple H-bonds with several different partners.

CONCLUSIONS

Opioid drugs are of central interest to the treatment of pain, and description of how different opioid drugs interact with opioid receptors and other molecules may assist with the design of new drugs. Atomistic simulations of opioid binding to membrane-embedded receptors are potentially valuable as they might lead to a detailed picture of how opioid drugs bind and unbind at receptor interfaces.

Accurate force-field parameters are required for reliable numerical simulations. A severe limitation in deriving accurate force-field parameters is the large number of QM and MM computations involved in the iterative procedure for parametrization of bonded and nonbonded interactions included in the force-field equation. To overcome this challenge, and since the dynamics of drug−receptor interactions at room temperature would be largely governed by the soft dihedral angles associated with relatively small energetic penalties, and by Coulomb interactions, we focused on deriving torsional potentials for flexible regions and atomic partial charges.

The force-field parameters we derived for morphine, heroin, and oliceridine allow a very good description of the structures of the drug molecules (Figure 9). Short QM MD simulations of the drugs in the presence of water molecules indicate that, for most H-bonding sites, water interaction distances are well described by the force field. Likewise, prolonged MM MD simulations of the isolated drug molecules suggest overall good qualitative agreement with the intrinsic torsional barriers and that the dynamics of flexible linker regions will be shaped by the interplay between the intrinsic torsional potential and intramolecular interactions. Together with the force-field parameters we presented recently for fentanyl and a fluorinated fentanyl derivative,[14] the force-field parameters we report here

https://doi.org/10.1021/acs.jcim.1c00667
J. Chem. Inf. Model. 2021, 61, 3964−3977

enable systematic computations of the binding of opioid receptors to different opioid drugs.

The force-field parametrization we presented here for opioid drugs underlines the importance of a careful parametrization protocol that ensures that the conformational dynamics and nonbonded interactions of the druglike molecule are represented accurately. Oliceridine is a highly flexible molecule in which the thiopene moiety connects to the spiro and pyridine rings via a five-bond linker; the thiopene moiety is further bound to an ether moiety (Figure 1D). The torsional potentials describing the orientation of the ether moiety relative to the thiopene ring and the orientation of thiopene relative to the spiro and pyridine rings were poorly represented within the automated methodology, such that numerical simulations performed with generic force-field parameters would have led to incorrect conformational dynamics of oliceridine. Importantly, for all opioid drug molecules we parametrized here, water interaction energy computations revealed the generic partial atomic charges required optimization for nonbonded interactions to be described correctly.

The automated protocol we used for the optimization of partial atomic charges makes the derivation of partial charges efficient even for relatively large molecules.

QM MD simulations of drug molecules augment the computations performed within the standard CGenFF protocol for force-field parametrization. We found the QM MD simulations on isolated compounds valuable as guidance to identify, from the time series of the dihedral angle values, flexible dihedral angles that might require careful inspection and optimization of the torsional potentials. The QM MD simulations of the drug molecules in the presence of water molecules inform on water interactions that might be sampled by the molecule as it is allowed to sample different conformations at room temperature.

■ ASSOCIATED CONTENT

Supporting Information

The Supporting Information is available free of charge at https://pubs.acs.org/doi/10.1021/acs.jcim.1c00667.

Tables S1−S3, high-penalty parameters for morphine, heroin, and oliceridine; Table S4, water interactions of heroin-2; Table S5, list of figures where selected atoms of opioid drugs are labeled; Figure S1, starting structures of heroin-1 and heroin-2; Figure S2, schematic representations of morphine, heroin, fentanyl, and oliceridine, with all atoms labeled; Figures S3−S7, analyses of the dynamics of isolated opioid drugs; Figure S8, schematic representation of the angle between ring planes of fentanyl and oliceridine; Figure S9, intramolecular H-bonding in oliceridine; Figures S10−S12, data analyses for PES computations; Figures S13−S25, data analyses for MM MD simulations of isolated opioid drugs; Figures S26−S32, data analyses of water interactions of opioid drugs in test B3LYP MD simulations; stream files containing the topologies and force-field parameters for morphine, heroin, and oliceridine (PDF)

■ AUTHOR INFORMATION

Corresponding Author

Ana-Nicoleta Bondar − *Theoretical Molecular Biophysics Group, Department of Physics, Freie Universität Berlin, D-14195 Berlin, Germany; Faculty of Physics, University of Bucharest, Măgurele 077125, Romania; Institute for Neuroscience and Medicine and Institute for Advanced Simulations (IAS-5/INM-9), Computational Biomedicine, Forschungszentrum Jülich, 52425 Jülich, Germany;* orcid.org/0000-0003-2636-9773; Email: nbondar@fizica.unibuc.ro

Authors

Thomas Giannos − *Theoretical Molecular Biophysics Group, Department of Physics, Freie Universität Berlin, D-14195 Berlin, Germany*

Samo Lešnik − *Laboratory of Physical Chemistry and Chemical Thermodynamics, Faculty of Chemistry and Chemical Engineering, University of Maribor, SI-2000 Maribor, Slovenia*

Urban Bren − *Laboratory of Physical Chemistry and Chemical Thermodynamics, Faculty of Chemistry and Chemical Engineering, University of Maribor, SI-2000 Maribor, Slovenia; Faculty of Mathematics, Natural Sciences and Information Technologies, University of Primorska, SI-6000 Koper, Slovenia;* orcid.org/0000-0002-8806-3019

Milan Hodošček − *Theory Department, National Institute of Chemistry Slovenia, SI-1001 Ljubljana, Slovenia;* orcid.org/0000-0002-6728-9318

Tatiana Domratcheva − *Department of Chemistry, Lomonosov Moscow State University, Moscow 119991, Russia; Department of Biomolecular Mechanisms, Max-Planck-Institut fur Medizinische Forschung, D-69120 Heidelberg, Germany;* orcid.org/0000-0002-7001-1114

Complete contact information is available at: https://pubs.acs.org/10.1021/acs.jcim.1c00667

Author Contributions

◆T.G. and S.L. contributed equally.

Notes

The authors declare no competing financial interest.

Computations were performed with publicly available software ORCA and CHARMM and with license-based software Gaussian. The force-field parameters developed in this work are included in the Supporting Information associated with this work. The Python script to optimize partial atomic charges, and the CHARMM topology, parameter, and stream files for the opioid drugs parametrized here, are available at GitLab: https://gitlab.com/samolesnik/partial-charge-optimization.

■ ACKNOWLEDGMENTS

Computations were performed on the ZEDAT computer cluster of the Freie Universität Berlin, the local computer cluster of the Department of Physics of the FU Berlin, and the CROW cluster of the National Institute of Chemistry Ljubljana, Slovenia. A.-N.B. acknowledges financial support from the Freie Universität Berlin. U.B. and S.L. acknowledge financial support from the Slovenian Ministry of Science and Education through project grant C3330-19-952021 and from the Slovenian Research Agency program and project grants P2-0046 and J1-2471. M.H. acknowledges financial support from the Slovenian Research Agency program grant L7-8269.

REFERENCES

(1) Rosenbaum, D. M.; Rasmussen, S. G. F.; Kobilka, B. K. The Structure and Function of G-Protein-Coupled Receptors. *Nature* **2009**, *459*, 356−363.

(2) Benyamin, R.; Trescot, A. M.; Datta, S.; Buenaventura, R.; Adlaka, R.; Sehgal, N.; Glaser, S. E.; Vallejo, R. Opioid Complications and Side Effects. *Pain Physician* **2008**, *11*, S105−S120.

(3) del Vecchio, G.; Spahn, V.; Stein, C. Novel Opioid Analgesics and Side Effects. *ACS Chem. Neurosci.* **2017**, *8*, 1638−1640.

(4) Patrick, G. L. *An Introduction to Medicinal Chemistry*, 5th ed.; Oxford University Press: Oxford, UK, 2013.

(5) Glare, P.; Walsh, D. A.; Sheehan, D. The Adverse Effects of Morphine: A Prospective Study of Common Symptoms During Repeated Dosing of Chronic Cancer Pain. *Am. J. Hospice Palliative Med.* **2006**, *23*, 229−235.

(6) Muijers, R. B. R.; Wagstaff, A. J. Transdermal Fentanyl. An Updated Review of its Pharmacological Properties and Therapeutic Efficacy in Chronic Cancer Pain Control. *Drugs* **2001**, *61*, 2289−2307.

(7) Dewire, S. M.; Yamashita, D. S.; Rominger, D. H.; Liu, G.; Cowan, C. L.; Graczyk, T. M.; Chen, X.-T.; Pitis, P. M.; Gotchev, D.; Yuan, C.; Koblish, M.; Lark, M. W.; Violin, J. D. A G Protein-Biased Ligand at the μ-Opioid Receptor is Potently Analgesic With Reduced Gastrointestinal and Respiratory Dysfunction Compared to Morphine. *J. Pharmacol. Exp. Ther.* **2013**, *344*, 708−717.

(8) Markham, A. Oliceridine: First Approval. *Drugs* **2020**, *80*, 1739−1744.

(9) Gillis, A.; Gondin, A. B.; Kliewer, A.; Sanchez, J.; Lim, H. D.; Alamein, C.; Manandhar, P.; Santiago, M.; Fritzwanker, S.; Schmiedel, F.; Katte, T. A.; Reekie, T.; Grimsey, N. L.; Kassiou, M.; Kellam, B.; Krasel, C.; Halls, M. L.; Connor, M.; Lane, J. R.; Schulz, S.; Christie, M. J.; Canals, M. Low Intrinsic Efficacy for G Protein Activation Can Explain the Improved Side Effect Profiles of New Opioid Agonists. *Sci. Signal.* **2020**, *13*, No. eaaz3140.

(10) Gelbrich, T.; Braun, D. E.; Griesser, U. J. Stable Polymorph of Morphine. *Acta Crystallogr., Sect. E* **2013**, *69*, o2.

(11) Deschamps, J. R.; George, C.; Filippen-Anderson, J. L. A Diacetylmorphine Polymorph. *Acta Crystallogr., Sect. C* **1996**, *52*, 698−700.

(12) Ogawa, N.; Nagase, H.; Endo, T.; Loftsson, T.; Ueda, H. Crystal Structure of Fentanyl Base. *X-Ray Struct. Anal. Online* **2009**, *25*, 83−84.

(13) Spahn, V.; del Vecchio, G.; Labuz, D.; Rodriguez-Gaztelumendi, A.; Massaly, N.; Temp, J.; Durmaz, V.; Sabri, P.; Reidelbach, M.; Machelska, H.; Weber, M.; Stein, C. A Nontoxic Pain Killer Designed by Modeling of Pathological Receptor Conformations. *Science* **2017**, *355*, 966−969.

(14) Lešnik, S.; Hodošček, M.; Bren, U.; Stein, C.; Bondar, A.-N. Potential Energy Function for Fentanyl-Based Opioid Pain Killers. *J. Chem. Inf. Model.* **2020**, *60*, 3566−3576.

(15) Brooks, B. R.; Bruccoleri, R. E.; Olafson, B. D.; States, D. J.; Swaminathan, S.; Karplus, M. CHARMM: A Program for Macromolecular Energy, Minimization, and Dynamics Calculations. *J. Comput. Chem.* **1983**, *4*, 187−217.

(16) Vanommeslaeghe, K.; Hatcher, E.; Acharya, C.; Kundu, S.; Zhong, S.; Shim, J.; Darian, E.; Guvench, O.; Lopes, P.; Vorobyov, I.; MacKerell, A. D., Jr. CHARMM Additive General Force Field: A Force Field for Drug-like Molecules Compatible with the CHARMM All-atom Additive Biological Force Fields. *J. Comput. Chem.* **2010**, *31*, 671−690.

(17) Hanwell, M. D.; Curtis, D. E.; Lonie, D. C.; Vandermeersch, T.; Zurek, E.; Hutchison, G. R. Avogadro: An Open-Source Molecular Builder and Visualization Tool. *J. Cheminform.* **2012**, *4*, No. 17.

(18) Li, J.-G.; Chen, C.; Yin, J.; Rice, K.; Zhang, Y.; Matecka, D.; de Riel, J. K.; DesJarlais, R. L.; Liu-Chen, L.-Y. Asp147 in the Third Transmembrane Helix of the Rat μ Opioid Receptor Forms Ion-Pairing with Morphine and Naltrexone. *Life Sci.* **1999**, *65*, 175−185.

(19) Dosen-Micovic, L.; Ivanovic, M.; Micovic, V. Steric Interactions and the Activity of Fentanyl Analogues at the Mu-Opioid Receptor. *Bioorg. Med. Chem.* **2006**, *14*, 2887−2895.

(20) Frisch, M. J.; Trucks, G. W.; Schlegel, H. B.; Scuseria, G. E.; Robb, M. A.; Cheeseman, J. R.; Scalmani, G.; Barone, V.; Mennucci, B.; Petersson, G. A.; Nakatsuji, H.; Caricato, M.; Li, X.; Hratchian, H. P.; Izmaylov, A. F.; Bloino, J.; Zheng, G.; Sonnenberg, J. L.; Hada, M.; Ehara, M.; Toyota, K.; Fukuda, R.; Hasegawa, J.; Ishida, M.; Nakajima, T.; Honda, Y.; Kitao, O.; Nakai, H.; Vreven, T.; Montgomery, J. A., Jr.; Peralta, J. E.; Ogliaro, F.; Beapark, M.; Heyd, J. J.; Brothers, E.; Kudin, K. N.; Staroverov, V. N.; Kobayashi, R.; Normand, J.; Raghavachari, K.; Rendell, A.; Burant, J. C.; Iyengar, S. S.; Tomasi, J.; Cossi, M.; Rega, N.; Millam, J. M.; Klene, M.; Knox, J. E.; Cross, J. B.; Bakken, V.; Adamo, C.; Jaramillo, J.; Gomperts, R.; Stratmann, R. E.; Yazyev, O.; Austin, A. J.; Cammi, R.; Pomelli, C.; Ochterski, J. W.; Martin, R. L.; Morokuma, K.; Zakrzewski, V. G.; Voth, G. A.; Salvador, P.; Dannenberg, J. J.; Dapprich, S.; Daniels, A. D.; Farkas, O.; Foresman, J. B.; Ortiz, J. V.; Ciosliwski, J.; Fox, D. J. *Gaussian 16*; Gaussian, Inc.: Wallingford, CT, 2009.

(21) Neese, F. The ORCA Program System. *Wiley Interdiscip. Rev.: Comput. Mol. Sci.* **2012**, *2*, 73−78.

(22) Jo, S.; Kim, T.; Iyer, V. G.; Im, W. CHARMM-GUI: A Web-Based Graphical User Interface for CHARMM. *J. Comput. Chem.* **2008**, *29*, 1859−1865.

(23) Humphrey, W.; Dalke, W.; Schulten, K. VMD: Visual Molecular Dynamics. *J. Mol. Graphics* **1996**, *14*, 33−38.

(24) MacKerell, A. D., Jr.; Bashford, D.; Bellot, M.; Dunbrack, R. L.; Evanseck, J. D.; Field, M. J.; Fischer, S.; Gao, J.; Guo, H.; Ha, S.; Joseph-McCarthy, D.; Kuchnir, L.; Kuczera, K.; Lau, F. T. K.; Mattos, C.; Michnick, S.; Ngo, T.; Nguyen, D. T.; Prodhom, B.; Reiher, W. E. I.; Roux, B.; Schlenkrich, M.; Smith, J. C.; Stote, R.; Straub, J.; Watanabe, M.; Wiorkiewicz-Kuczera, J.; Yin, D.; Karplus, M. All-Atom Empirical Potential for Molecular Modeling and Dynamics Studies of Proteins. *J. Phys. Chem. B* **1998**, *102*, 3586−3616.

(25) MacKerell, A. D., Jr.; Feig, M.; Brooks, C. L. I. Extending the Treatment of Backbone Energetics in Protein Force Fields: Limitations of Gas-Phase Quantum Mechanics in Reproducing Protein Conformational Distributions in Molecular Dynamics Simulations. *J. Comput. Chem.* **2004**, *25*, 1400−1415.

(26) Nosé, S. A Molecular Dynamics Method for Simulations in the Canonical Ensemble. *Mol. Phys.* **1984**, *52*, 255−268.

(27) Vanommeslaeghe, K.; MacKerell, A. D., Jr. Automation of the CHARMM General Force Field (CGenFF) I: Bond Perception and Atom Typing. *J. Chem. Inf. Model.* **2012**, *52*, 3144−3154.

(28) Vanommeslaeghe, K.; Raman, E. P.; MacKerell, A. D., Jr. Automation of the CHARMM General Force Field (CGenFF) II: Assignment of Bonded Parameters and Partial Atomic Charges. *J. Chem. Inf. Model.* **2012**, *52*, 3155−3168.

(29) Jorgensen, W. L.; Chandrasekhar, J.; Madura, J. D.; Impey, R. W.; Klein, M. L. Comparison of Simple Potential Functions for Simulating Liquid Water. *J. Chem. Phys.* **1983**, *79*, 926−935.

(30) Mayne, C. G.; Saam, J.; Schulten, K.; Tajkhorshid, E.; Gumbart, J. C. Rapid Parametrization of Small Molecules Using the Force Field Toolkit. *J. Comput. Chem.* **2013**, *34*, 2757−2770.

(31) Wang, J.; Kollman, P. A. Automatic Parametrization of Force Field by Systematic Search and Genetic Algorithms. *J. Comput. Chem.* **2001**, *22*, 1219−1228.

(32) Wang, L.-P.; Chen, J.-H.; Voorhis, T. V. Systematic Parametrization of Polarizable Force Fields from Quantum Chemistry Data. *J. Chem. Theor. Comput.* **2013**, *9*, 452−460.

(33) Bertalan, É.; Lešnik, S.; Bren, U.; Bondar, A.-N. Protein-Water Hydrogen-Bond Networks of G Protein-Coupled Receptors: Graph-Based Analyses of Static Structures and Molecular Dynamics. *J. Struct. Biol.* **2020**, *212*, No. 107634.

https://doi.org/10.1021/acs.jcim.1c00667
J. Chem. Inf. Model. 2021, 61, 3964−3977